

STRESS AND STRAIN MONITORING OF REINFORCED-SOIL TEST WALL

Khalid Farrag, Ph.D., P.E. (Corresponding author)
Manager, Civil & Geotechnical Research
GTI
1700 S. Mount Prospect Road
Des Plaines, IL 60018
Phone: (847) 768-0803
Fax: (847) 768-0569
E-Mail: Khalid.farrag@gastechnology.org

Murad Abu-Farsakh, Ph.D., P.E.
Research Assistant Professor
Louisiana Transportation Research Center
Louisiana State University
4101 Gourrier Ave.
Baton Rouge, LA 70803
Phone: (225) 767-9147

And

Mark Morvant, P.E.
Geotechnical and Pavement Research Administrator
Louisiana Transportation Research Center
4101 Gourrier Ave.
Baton Rouge, LA 70803
Phone (225) 767-9124

Submitted to:

83th Transportation Research Board Annual Meeting
January 12-16, 2004
Washington, D.C.

STRESS AND STRAIN MONITORING OF REINFORCED-SOIL TEST WALL

ABSTRACT

The measurements of stresses and strains in a full-scale reinforced test wall are presented. The test wall was constructed to evaluate the design procedure and performance of geosynthetic-reinforced walls constructed with silty-clay marginal backfill over soft clay foundation. The instrumentation program consisted of monitoring wall deformation, foundation settlement, strains along the reinforcement, vertical and horizontal stresses in the soil and at the facing, and pore water pressure under the wall. This paper focuses on presenting the instrumentations and measurements of wall deformation, soil stresses, and reinforcement strains during and after construction. The strains and deformation measurements were utilized in predicting the reinforcement loads and the state of stresses in the reinforced-soil system.

The wall consisted of three sections reinforced with various geogrid reinforcement types and spacing. The first section was built with closely spaced low strength geogrid while the second section was constructed using higher strength geogrid at a maximum vertical spacing. The reinforcement and spacing of the third section were based on standard design procedures.

Deformations along the reinforcement were monitored using strain gauges installed at several locations along the geogrid length. The deformations of the wall and the magnitudes and distributions of strains varied in the three wall sections. The strains in the reinforcement were utilized in evaluating the progressive development of stresses during construction and the corresponding slip surfaces.

The concept of normalizing reinforcement stress ($T_{\max} / \gamma h S_h S_v$) was useful in defining the relative 'rigidity' of the wall and in determining the horizontal stress coefficient of the wall (K). The results show that the locus of maximum stresses in the reinforcement did not correspond to the $(45 + \phi / 2)$ line and varied according to the reinforcement rigidity. A comparison was made between the measured and predicted maximum tensile loads (T_{\max}) in the reinforcements. The results indicated that the loads predicted by the K_o -Stiffness method were close to the measured loads than the Simplified AASHTO method.

INTRODUCTION

A full-scale reinforced test wall was constructed at the Louisiana Transportation Research Center (LTRC) in order to evaluate the performance of geosynthetics-reinforced walls constructed with low quality marginal backfill. The test wall was 20 ft (6 m) high and 160 ft (48 m) long with modular block facing. It consisted of three test sections reinforced with various geogrids. The first section of the wall (Section 1) was constructed using low strength geogrid placed at a minimum vertical spacing of 16 inches (0.4 m). Section 2 was constructed using higher strength geogrid placed at a maximum vertical spacing of 40 inches (1 m). The internal stability design of these two sections incorporated factors of safety of unity for construction damage and material degradation. A factor of safety of 3 was taken for creep loads in order to obtain measurable deformations. Section 3 was designed according to AASHTO standard specifications [1] and its vertical spacing was selected so as to perform pullout tests on dummy specimens placed between the main reinforcement. Details of the construction and instrumentation of the wall are in reference [2].

The instrumentations of the test wall were used in monitoring the ‘during construction’ and ‘short-term’ soil deformations, the mobilized strains in the reinforcement, earth pressures in the soil and at the facing, and the settlement of the soft soil foundations. Accordingly, the instrumentation program included survey points, inclinometers, and settlement plates to measure deformations, earth pressure cells to monitor soil stresses, and strain gauges and extensometers to monitor strains in the reinforcement.

The two main objectives of monitoring soil stresses and reinforcement strains in the test wall were:

- 1) Evaluate the effect of reinforcement stiffness and spacing on the shape of the failure surface in the wall.
- 2) Determine the loads in the reinforcement layers in each of the wall test sections

The loads in the reinforcement were determined from the measurements of strain gauges at various locations along the length of each reinforcement layer. The results of strain measurements in the reinforcement were used in evaluating the effect of reinforcement stiffness and spacing on the shape of the failure surface and on the distribution and magnitude of stresses in reinforcement layers.

PROPERTIES OF THE WALL TEST SECTIONS

The test wall was constructed using silty-clay backfill of medium plasticity ($PI = 15$). This soil had 72% silt, 19% clay, maximum dry unit weight of 105 lb/ft^3 , and optimum moisture content of 18%. An angle of internal friction (ϕ) = 24° and a cohesion (C) = 30 psf were obtained from undrained direct shear tests. Soil cohesion, however, was not included in the design of the test wall. The wall had a constant height of 20 ft (6 m). The height of the wall was uniform for a length of 100 ft (30 m) and then was sloped down at one end for a length of about 60 ft (18 m) in a slope of 3 to 1 in order to facilitate the construction of the wall. Figure 1 shows a view of the vertical wall.

The vertical wall consisted of three sections reinforced with various geogrid types and spacing. Section 1 was reinforced with a relatively low strength geogrid (Tensar UX-750) not commonly used in wall reinforcement. The geogrid was placed at minimum vertical spacing of two modular blocks (16 inches). Section 2 of the wall was constructed with relatively strong geogrid (Tensar UX-1400) placed at a maximum spacing of 5 modular blocks (40 inches). Section 3 of the vertical wall was reinforced with stronger geogrid (Tensar UX-1500) and was used in performing field pullout tests on various geosynthetic specimens placed between the main reinforcement. Figures 2, 3, and 4 show the sections the test wall. Table 1 shows the properties of the geogrid reinforcement in each section.

The facing of section 1 consisted of compact type 'Keystone' modular blocks of 8 inches high, 8 inches wide, and 12 inches deep while the facing of sections 2 and 3 were standard size blocks of height 8 inches, width 18 inches and depth of 21 inches.

MEASUREMENTS OF SOIL STRESSES

The development of soil stresses during construction was monitored using horizontal and vertical earth pressure cells. The cells were 'Geokon' semiconductor strain gauge type of 6 in. (15 cm) diameter and maximum pressure of 30 psi. The cells were placed in horizontal and vertical positions at the locations shown in Figures 2 through 4. The installation procedure consisted of excavating the soil in the locations of the cells after the compaction of the soil layer. A thin sand layer was placed around the cell in order to insure full soil contact and the soil was compacted over one foot of soil cover. Figure 5 shows the installation of earth pressure cells.

The calibration of the cells was performed in the laboratory by placing the cells in soils identical to the backfill used in the field. Vertical loads were applied on the top of the soil in a load-controlled test. The loads were applied using a loading plate of larger diameter than the cell in order to insure uniform pressure distribution above the surface of the cell.

The vertical earth pressures at elevations 4 ft and 12 ft from the base of the wall (cells 213 and 215 in figures 3 and 4) during and after construction are shown in figure 6. The measurements started after placing one lift of soil above the cells at their perspective levels. The theoretical vertical pressures at these two levels are also plotted in the figure for comparison. The theoretical lines were calculated by multiplying the heights of soil above the cells by the average soil unit weight of 120 pcf.

The results show that the measured earth pressures compared well with the theoretical values at the early stages of construction. At the end of construction, the measured vertical pressures reached only about 75 percent of the theoretical values. The low values at later stages of construction can be attributed to the settlement of the base soil under the wall, which resulted in soil movement and relaxation of soil pressure beneath the cells.

The horizontal pressures at the same elevations (cells 212 and 214 in figures 3 and 4) are shown in figure 7. The theoretical horizontal stress, based on the estimation of K_a from soil friction

angle, is also plotted in the figure. The results show that the horizontal stresses near the facing did not fully mobilize to their maximum values till after the end of construction.

The horizontal earth pressure at the base of the wall was monitored by earth pressure cells placed against the facing blocks (cells 247 and 248 in figures 2 and 3). The results in Figure 8 show that the stresses reached their theoretical valued at the end of construction. However, lower pressures were monitored in the few months after wall completion.

The results of horizontal pressure measurements show that the apparent coefficient of lateral earth pressure (σ_h/σ_v) varied along the height of the wall and near the wall base possibly as a result of the frictional resistance between the soil and facing blocks and the reduction of vertical earth pressure due to foundation settlement.

MEASUREMENTS OF STRAINS IN THE REINFORCEMENT

Installation of strain gauges on geosynthetics

Conventional design of reinforced-walls incorporates high factors of safety and, consequently, the strains measured in typical walls are usually low. Field measurements in walls [3, 4, and 5] showed that strains were in the range of 0.1 to 0.5 percent, with most of these strains occurring during construction. Model test walls in the laboratory are usually designed to demonstrate higher deformations till failure under controlled loading conditions [6, 7]. The LTRC test wall was designed with a low overall factor of safety in order to obtain measurable deformations in the test sections.

Strain gauges were used in monitoring reinforcement strains. A number of factors affect the survivability of strains gauges in field conditions. Most of these factors relate to construction damage and presence of ground water. Accordingly, a large number of measurement points were required to represent the elongation profile along the geogrid length. An approximately 150 strain gauges were installed in the 3 sections. Some gauges were installed in the same location to provide redundancy of the measurements. Strain measurements were also compared with the rod extensometer readings. About 110 gauges survived at the end construction period and about 50 percent of the gauges were working during the 4 months monitoring period after construction.

Several factors such as surface texture of the geosynthetic, strain level, dimensions of the geogrid ribs, and low self-temperature compensation of the geosynthetic material govern the selection of the gauges. Accordingly, various types and sizes of Micro-Measurement (MM) resistance strain gauges were used. Relatively large strain levels up to 5 percent were expected in the wall and an annealed constantan grid material (EP type) was selected for this purpose. The constantan alloy was supplied in a self-temperature compensated form (S-T-C) in order to match the thermal expansion coefficient of the material tested. A high S-T-C number of 40 was selected for the geosynthetics application. The gauges were supplied in polyimide packing in order to provide the large elongation capability. The length of the gauges varied from 0.25 inches to 2 inches. The relatively longer gauges were easier to install and they provided better heat dissipation. Table 2 lists the types of strain gauges used in the test wall.

The installation of gauges on the geosynthetics resulted in stiffening of the specimen at the location of the gauge. Proper selection of adhesive and coating materials may reduce this effect. However, strain gauges measure the local strains at the location of the gauge, which may differ from the overall strain at the section where strain measurement is desired. Accordingly, calibration of the gauges measurements was necessary in order to correlate the gauges readings to the actual strain along the specimen section.

Calibration was performed in unconfined extension tests. Extensometers were placed on the specimen and the gauges readings were correlated to machine travel and to the extensometers readings. The tests resulted in calibration factors ranging from 0.75 to 0.85 for the geogrid types in the test sections.

Strain Measurements in the Wall Test Sections

Strains measurements of the reinforcement in the three test sections are shown in Figures 9 through 11. The figures show the strain distribution along the reinforcement at selected layers and the locus of maximum strains in the wall. The performance of the three sections during constructions can be summarized as follows:

- Maximum reinforcement strains occurred in section 1 (weak geogrid – minimum spacing). Strain of 3.5 percent was mobilized in the bottom third of the section (layer D). In section 2 (strong geogrid – maximum spacing), the maximum strain of 2 percent was measured at mid-height of the wall (layer D). Maximum strain in section 3 was 1.2 percent and was at the bottom third of the wall height (layer C). The result of the inclinometer readings and survey of the wall facing also showed more deformations in section 1 and that it was more ‘flexible’ system than sections 2 and 3. Figure 12 shows the magnitudes of maximum strains for section 1 and 2 at various stages of construction.
- The locations of maximum strains in the reinforcement layers were usually defined at early stages of construction.
- The strain curves along the reinforcement had a defined peak at the lower layers of the wall. Maximum strains at the top layers were spread over a wider length of the reinforcement.
- The locus of maximum strains in the three sections formed an angle less than the theoretical K_a failure surface of angle $(45 + \phi/2)$.
- The strains at the facing were higher at the upper half of the wall and were negligible at the bottom half. Moreover, the strains near the facing in section 1 were almost equal to the maximum strain in the reinforcement.
- The settlement of the wall reached about 10 inches at the end of construction due to the consolidation of the soft foundation soil. Survey of elevations at the wall facing and measurements of horizontal inclinometers under the reinforced sections showed that the settlement was approximately uniform under the reinforced part of the sections (11 ft). Figure 13 shows the measurements of horizontal inclinometer under the wall. As

differential settlement was negligible under the facing and reinforced part of the wall, it can be concluded that the settlement of the wall did not have an effect on the strain measurements near the wall facing,

Estimation of Failure Surface

The critical failure surface is assumed to coincide with the locus of maximum strains in each layer. Strain measurements show that the locus of the slip surface differed in the three test sections. The locations of maximum strains are plotted in figure 14. The figure shows that maximum strains coincided with the $(45 + \phi/2)$ line only at the bottom halves of the sections. A bilinear slip surface represented the locus of maximum strains in sections 1. The locus of maximum strains in section 2 was at a constant distance from wall facing at mid-height of the wall. The maximum strains of section 3 formed a linear surface of an angle less than the $(45 + \phi/2)$ line.

Estimation of Reinforcement Stresses

The magnitude of the mobilized strains (and consequently, stresses) in the reinforcement depends mainly on the reinforcement strength, its spacing, and soil-reinforcement interaction properties. This dependency is demonstrated in the relationship:

$$T_{\max} = K (\gamma h) S_h S_v \quad (1)$$

Where T_{\max} is the maximum tensile stress mobilized in the reinforcement layer, K is the coefficient of the horizontal stresses mobilized in the reinforcement, γ is soil unit weight, h is soil height above the reinforcement, S_h is the horizontal spacing (equals one unit length for the geogrid), and S_v is the vertical spacing.

The coefficient K is the challenging factor in estimating stresses in reinforced walls and it depends primarily on the soil-reinforcement interaction properties and the extensibility of the reinforcement. The state-of-practice design procedures assume K to be equal to the active earth pressure K_a for extensible reinforcement [8, 9]. By rearranging equation 1, the value of K can be evaluated by plotting the normalized tensile stresses ($T_{\max} / \gamma h S_h S_v$) for each reinforcement layer as shown in Figure 15. In the figure, the values of T_{\max} were calculated from the measured strains and the stiffness modulus of the geogrids. The distribution of normalized stresses in the figure shows:

- Low tensile stresses are commonly developed at the first reinforcement layer near the wall base due to the effect of the rigid base soil, which restrain the horizontal deformation. This is consistent with many other measurements in the field and in model walls.
- The normalized stresses (or K) in section 1 increased with depth till a maximum value near the bottom third of its height. For section 2, the stresses were approximately uniform

throughout most of the wall height. The stresses in section 3 increased linearly with depth with values less than the theoretical K_a .

Comparison between Measured and Predicted T_{\max}

Maximum stresses in the reinforcement were compared with two methods used in the estimation of the reinforcement, namely; a simplified method [10] based on AASHTO procedures [8, 9] and K_o -Stiffness method [11].

The AASHTO simplified method estimates T_{\max} as in equation 1 with K defined as K_r and the value of K_r/K_a varying from one for flexible geosynthetics to 2.5 for metal bar mats and wire grids. The K_o -Stiffness method was developed by first assuming conventional earth pressure (using K_o) behind the wall. The distribution of T_{\max} is then determined empirically from case histories and analytical modeling. A trapezoidal distribution was obtained for geosynthetics walls and a factor D_{\max} was introduced to characterize this distribution.

A comparison between the maximum tensile loads T_{\max} from wall measurements and the values predicted from the two methods are presented in figures 16, 17 and 18 for the three test sections, respectively. In these figures, a K_r/K_a value of 1.2 was used in the simplified method.

The figures show that the loads predicted by the K_o -Stiffness method are closer to the measured reinforcement loads than the simplified method. The analysis also shows that the proper estimate of the stiffness of all wall components leads to more appropriate prediction of the state of stresses in the reinforcement.

CONCLUSIONS

The results of the instrumentation of the test wall demonstrated the performance of various design configurations of geometry and strength of geosynthetics in silty-clay soil. The paper focused on presenting the stress-strain measurements of in the three test sections of the vertical wall. Strain gauges could be utilized in estimating the state of stresses in the reinforcement, providing proper installation and calibration of the gauges.

The results showed that the distribution of reinforcement strength in the layers varied with the change of reinforcement stiffness and its density in the wall. The concept of normalizing the strength to the term $(T_{\max} / \gamma h S_h S_v)$ defined the relative 'rigidity' of the wall and in determining the horizontal stress coefficient of the wall (K).

The theoretical angle of slip surface $(45 + \phi/2)$ did not correspond to the stresses in the three test sections. The results of comparison between the measured and predicted T_{\max} indicated that the K_o -Stiffness method could predict the measured loads better than the Simplified method.

ACKNOWLEDGMENT

The research program was supported by the Louisiana Department of Transportation and Development (LA DOTD) and the Louisiana Transportation Research Center (LTRC). The geogrid reinforcement of the wall test sections was donated by TENSAR Earth Technologies, Inc. Keystone Southeast donated the modular blocks. The support and cooperation provided by these agencies is gratefully appreciated.

REFERENCES

1. *Standard Specifications of Highway Bridges*, AASHTO, 1992.
2. Farrag, K., and Morvant, M., *Evaluation of Interaction Properties of Geosynthetics in Cohesive Soils: LTRC Reinforced-Soil Test Wall*, Louisiana Transportation Research Center, Report No. 92-4GT, 2003.
3. Allen, T., Christopher, B., and Holtz, R., "Performance of a 12.6 m high geotextile wall in Seattle, Washington", Proceedings, International Symposium on Geosynthetic-Reinforced Soil Retaining Walls, Denver, 1991, pp. 81-100.
4. Bell, J.R., Barrett R.K., and Buckman, A.C., "Geotextile Earth-Reinforced Retaining Wall Tests: Glenwood Canyon", Transportation Research Record 916, 1983, pp. 59-69.
5. Simac, M.R., Christopher, B.R., and Bonczkiewiz, C., "Instrumented Field Performance of a 6 m geogrid soil Wall", 4th International Conference on Geotextiles, Geomembranes & Related Products, The Hague, 1990, pp. 53-59.
6. Wu, J. T., "Measured Behavior of Denver Wall", Proceedings, International Symposium on Geosynthetic-Reinforced Soil Retaining Walls, 1991, pp. 31-41.
7. Bathurst, R.J., "Instrumentation of Geogrid-Reinforced Soil Walls", Transportation Research Record 1277, 1990, pp. 102-111.
8. Elias, V., and Christopher, B., *Mechanically Stabilized Earth Walls and Reinforced Soil Slopes*, FHWA, Report No. FHWA-SA-96-071, 1997.
9. Holtz, R., Christopher, B., and Berg, R., *Geosynthetics Design and Construction Guidelines*, FHWA, Report No. FHWA HI-95-038, 1998.
10. Allen, T., Christopher, B.R., Elias V., and DiMaggio, J., (2001), "Development of the Simplified Method for Internal Stability Design of Mechanically Stabilized Earth Walls", *Final Research Report for the WSDOT & FHWA*, June 2001.
11. Allen, T. and Bathurst, R.J., "Prediction of Soil Reinforcement Loads in Mechanically Stabilized Earth (MSE) Walls", *Final Research Report Prepared for WSDOT*, Oct. 2001.

TABLE 1 - Properties of the Geogrid Reinforcement in the Test Sections (*)

Test Section	Geogrid Type	Vertical Spacing (inch)	Aperture (inch)	Tensile Modulus (E) (Kips/ft)	Ultimate Strength (lb/ft)
Section 1 [Weak Geogrid - Min. spacing]	Tensar UX-750	16	6	27	2,200
Section 2 [Strong Geogrid -Max. spacing]	Tensar UX-1400	40	13.25	75	--
Section 3 [Pullout section - Stronger Geogrid]	Tensar UX-1500	variable	13.36	90-100	7,800

(*) All values are in machine direction

TABLE 2 - List of strain gauges used in the geosynthetics instrumentation

Gauge type	Length (inch)	Width (inch)	Resistance (ohms)	Application
EP-08-250BG-120	0.25	0.125	120	(HDPE grid) UX-750
EP-40-250BF-350-L	0.25	0.125	350	UX-1400,UX-1500, and UX-1600
EP-08-20CBW-120	1.0	0.188	120	



Figure 1 - View of the LTRC test wall

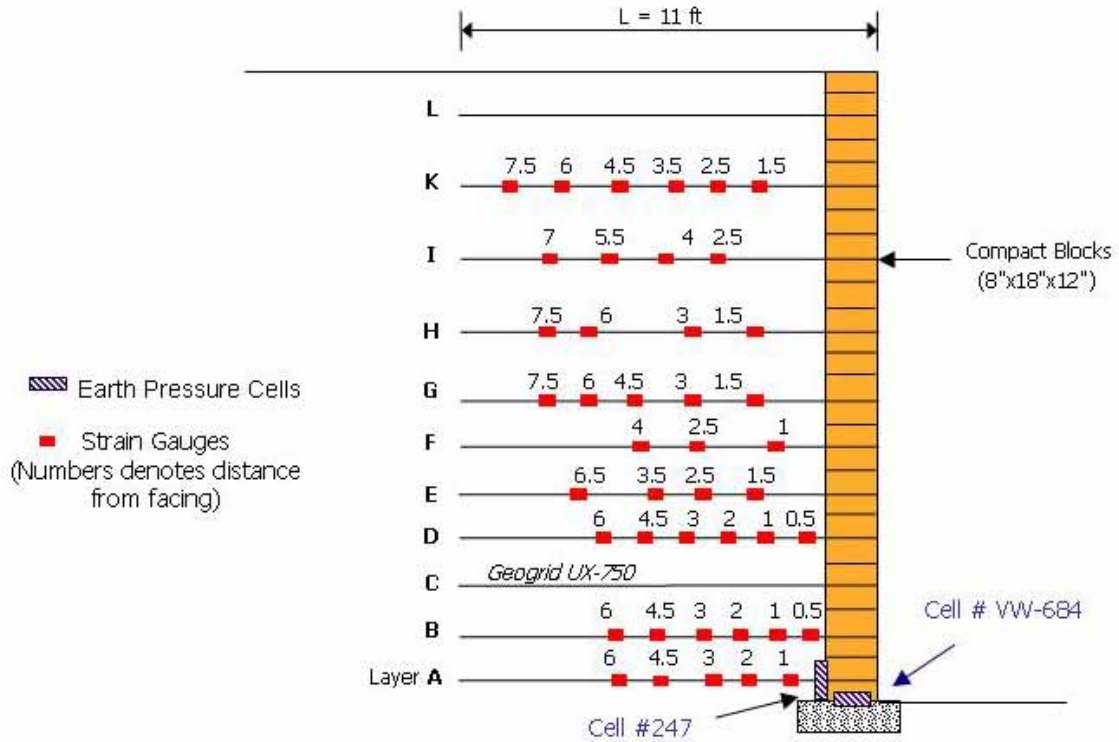


Figure 2 - Strain gauges and pressure cells of test section 1

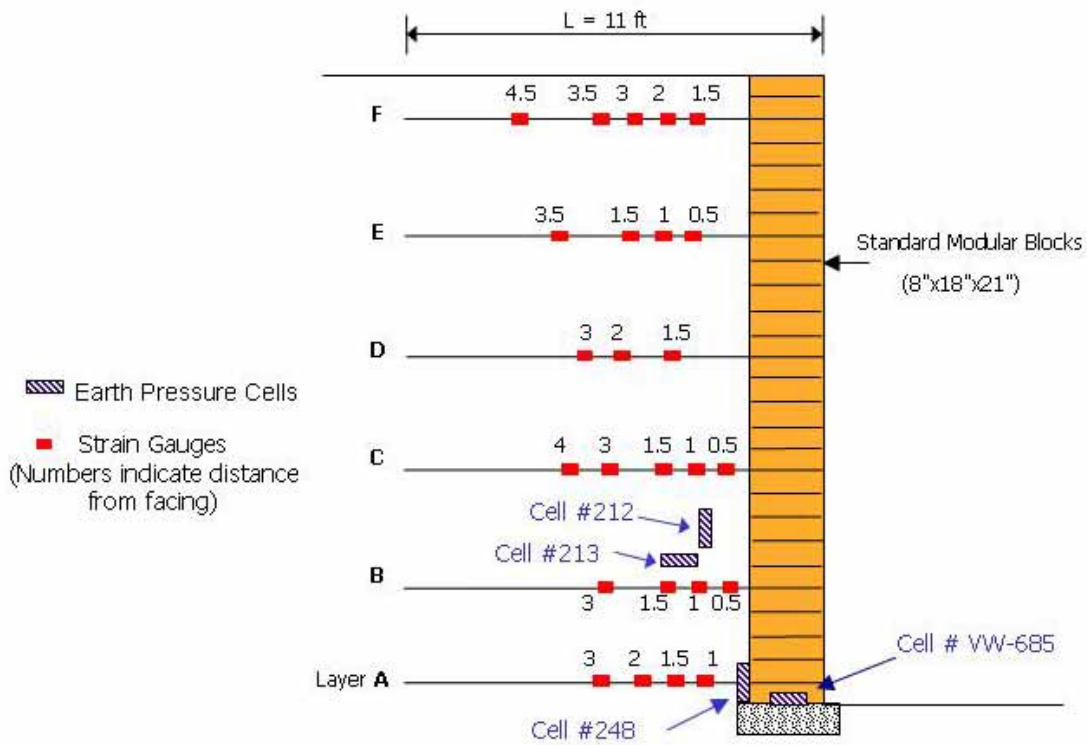


Figure 3 - Strain gauges and pressure cells of test section 2

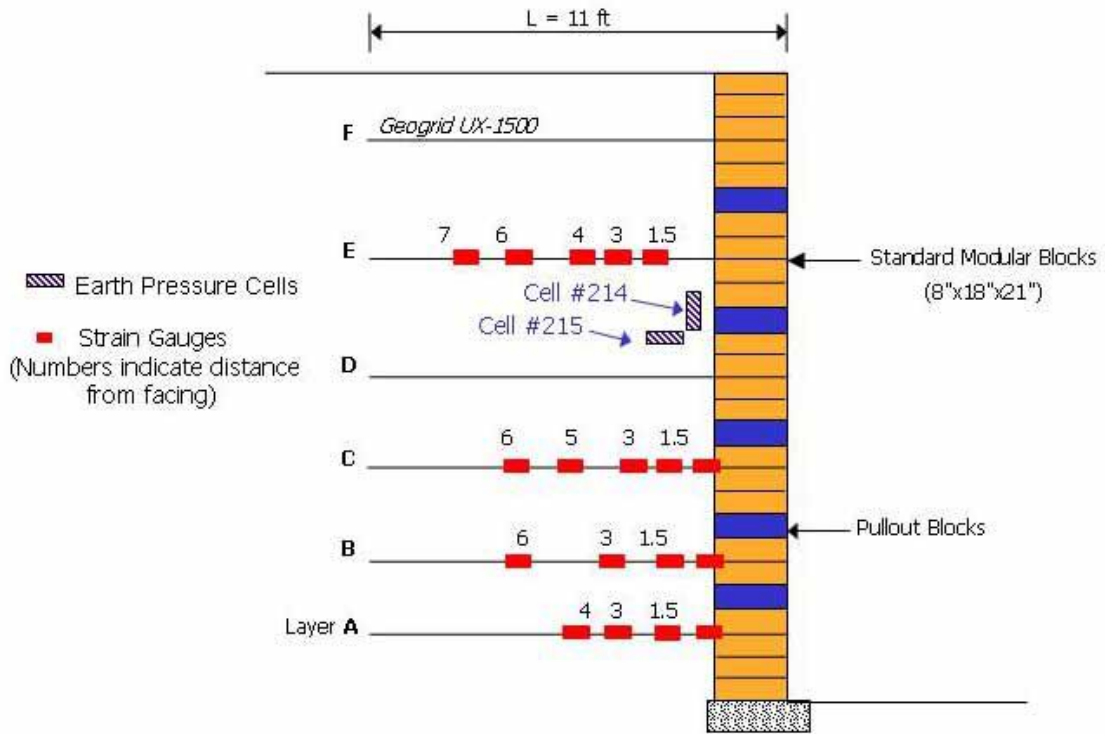


Figure 4 - Strain gauges and pressure cells of test section 3



Figure 5 - Installation of earth pressure cells behind the wall facing

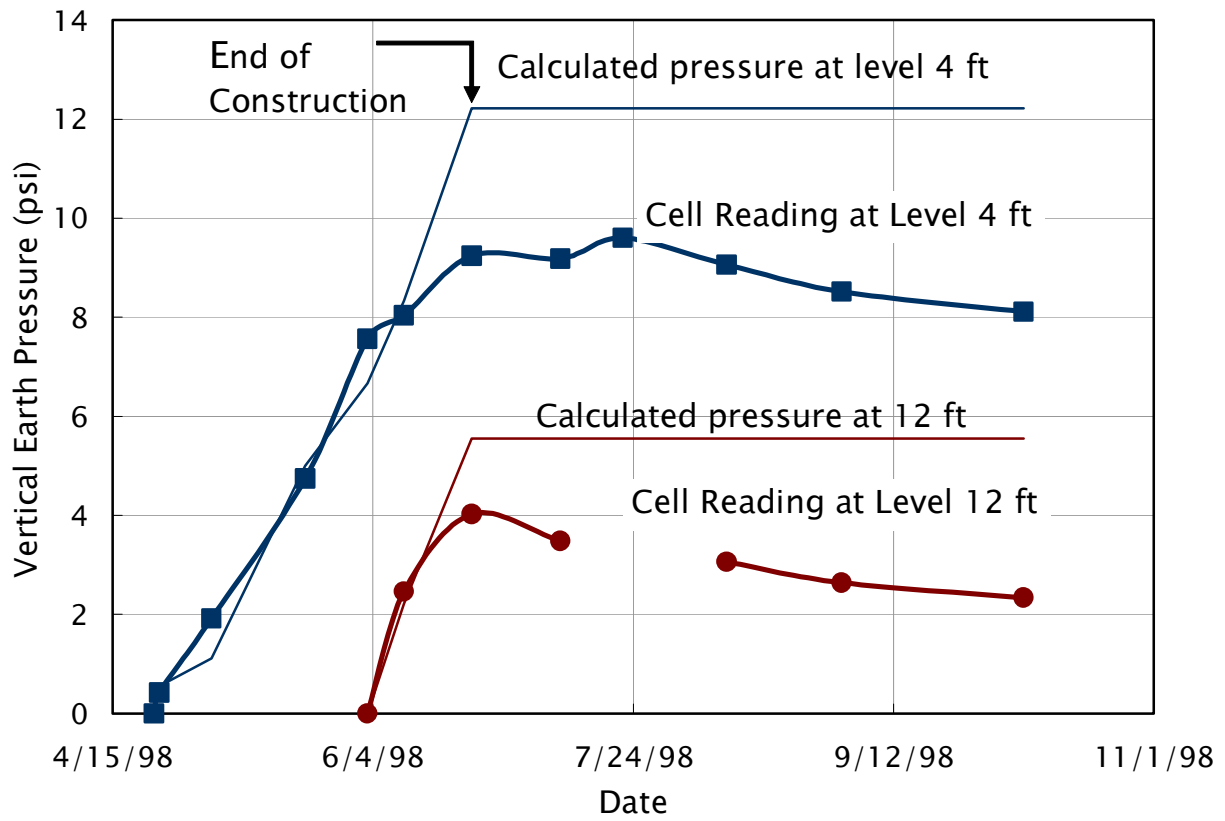


Figure 6 - Measured and calculated vertical earth pressure at two wall levels of 4 ft and 12 ft.

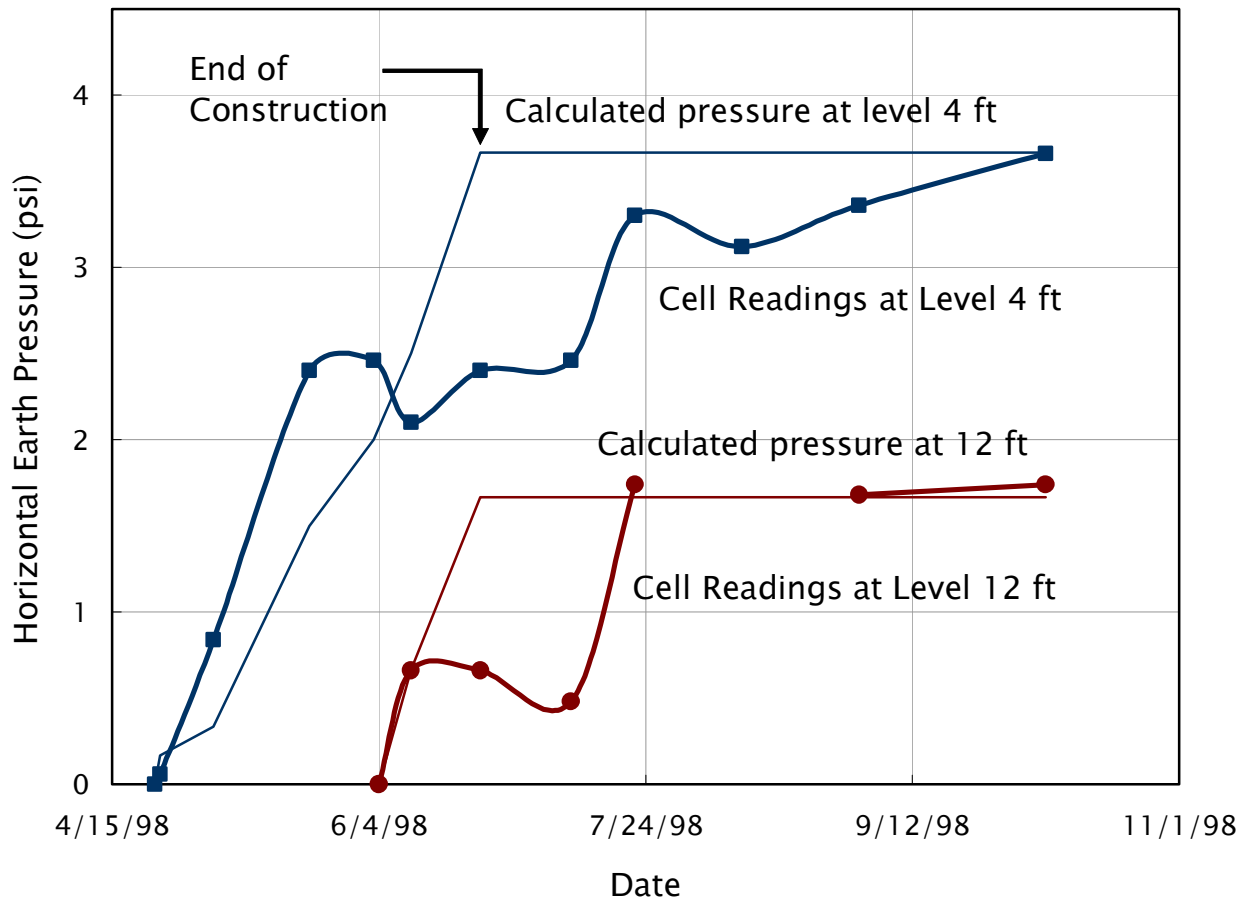


Figure 7 - Measured and calculated horizontal earth pressure at two wall levels of 4 ft and 12 ft.

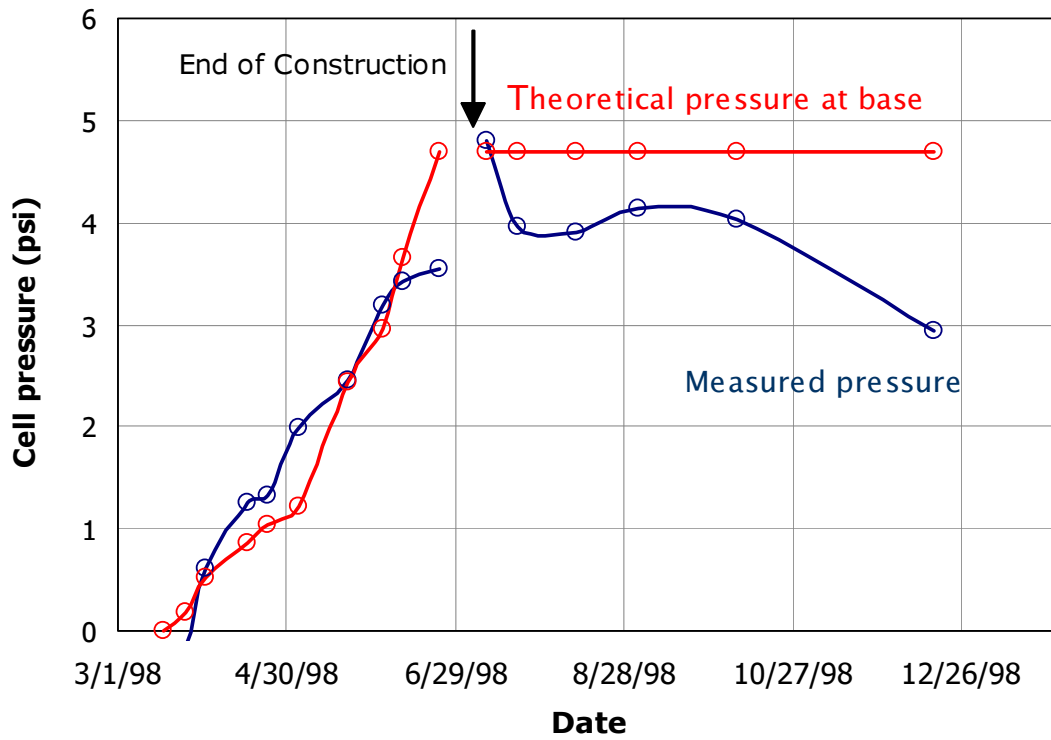


Figure 8 - Horizontal Earth pressure at the wall base

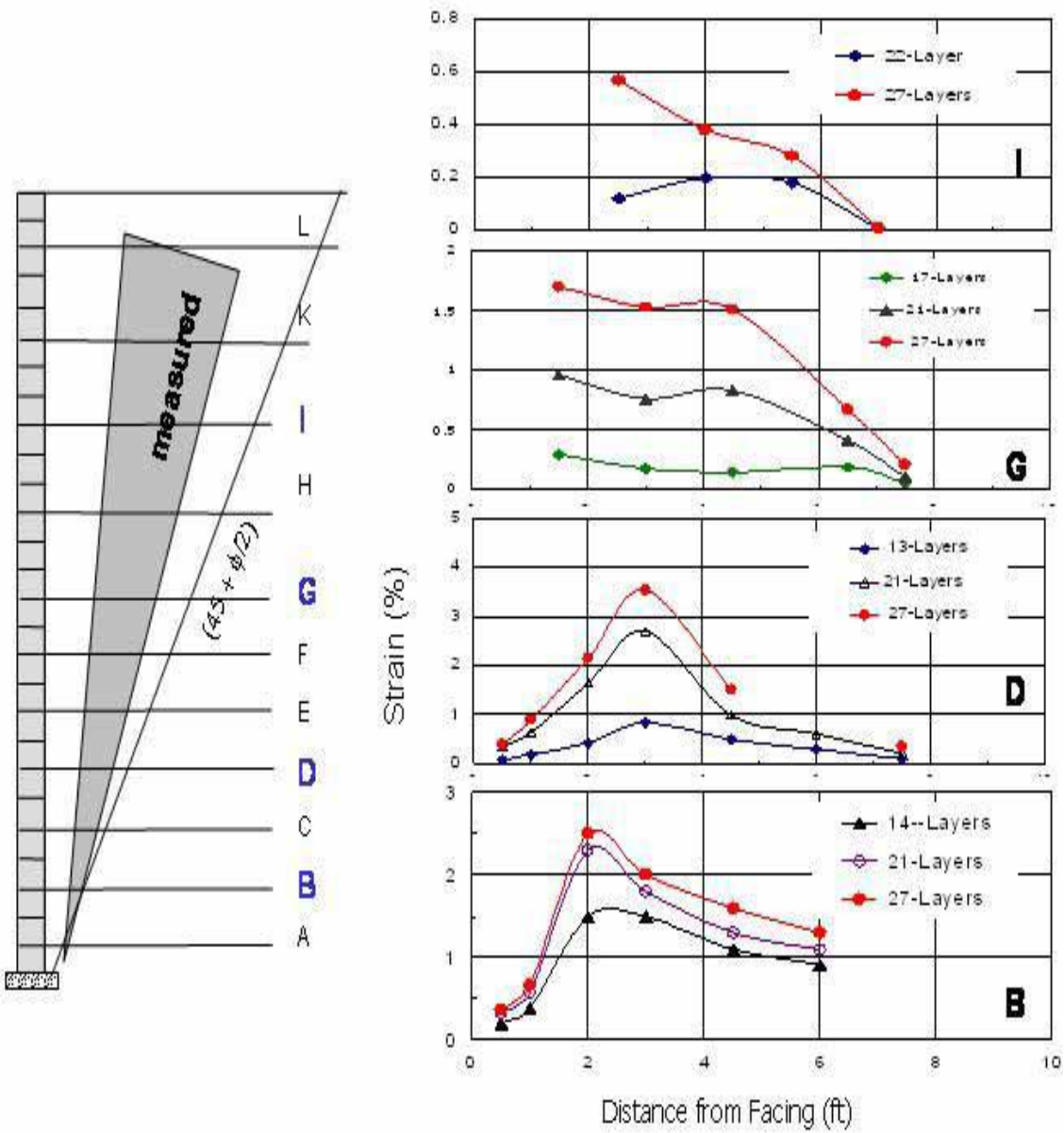


Figure 9 – Strain measurements and locations of maximum strains in test section 1

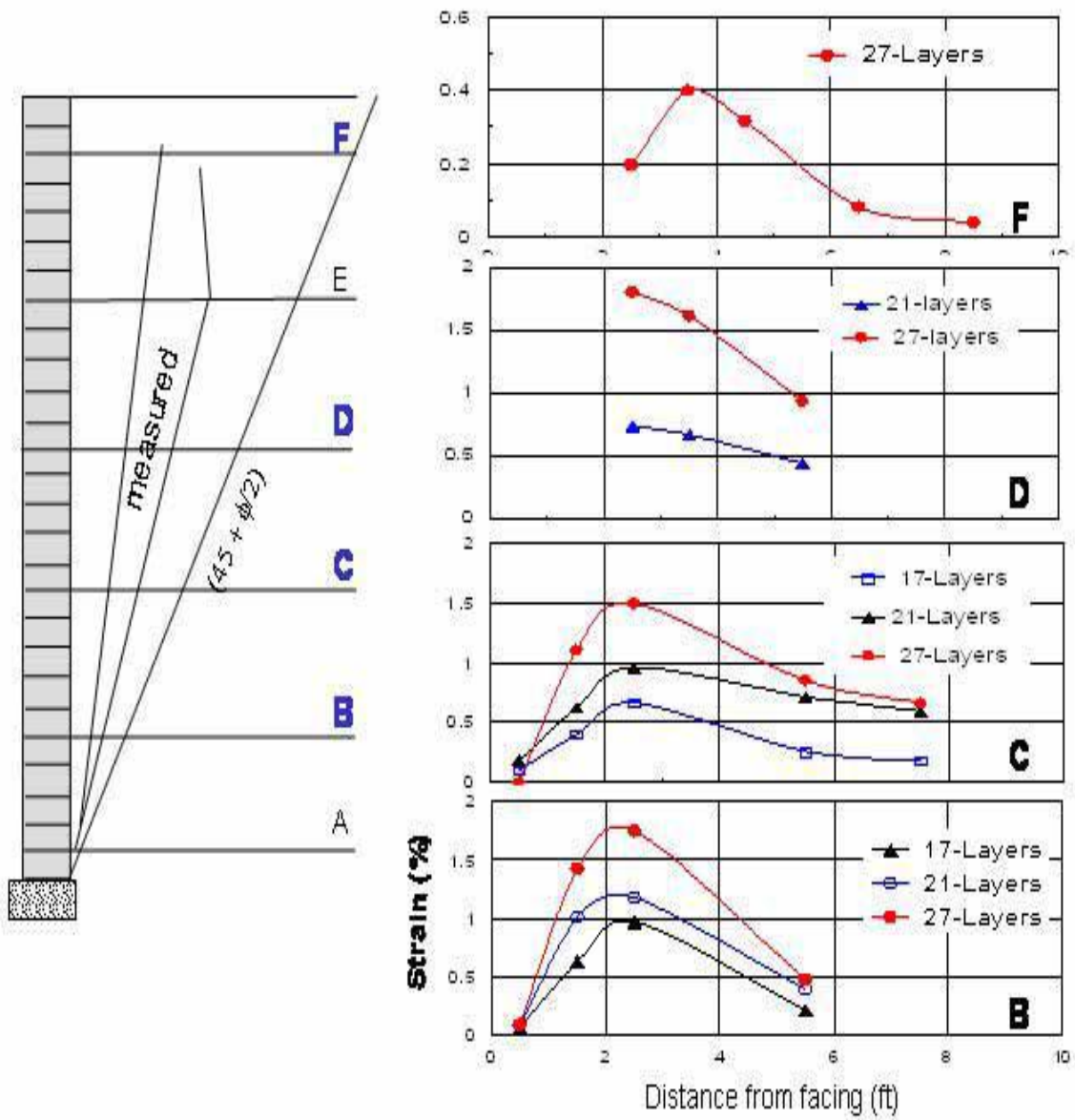


Figure 10 – Strain measurements and locations of maximum strains in test section 2

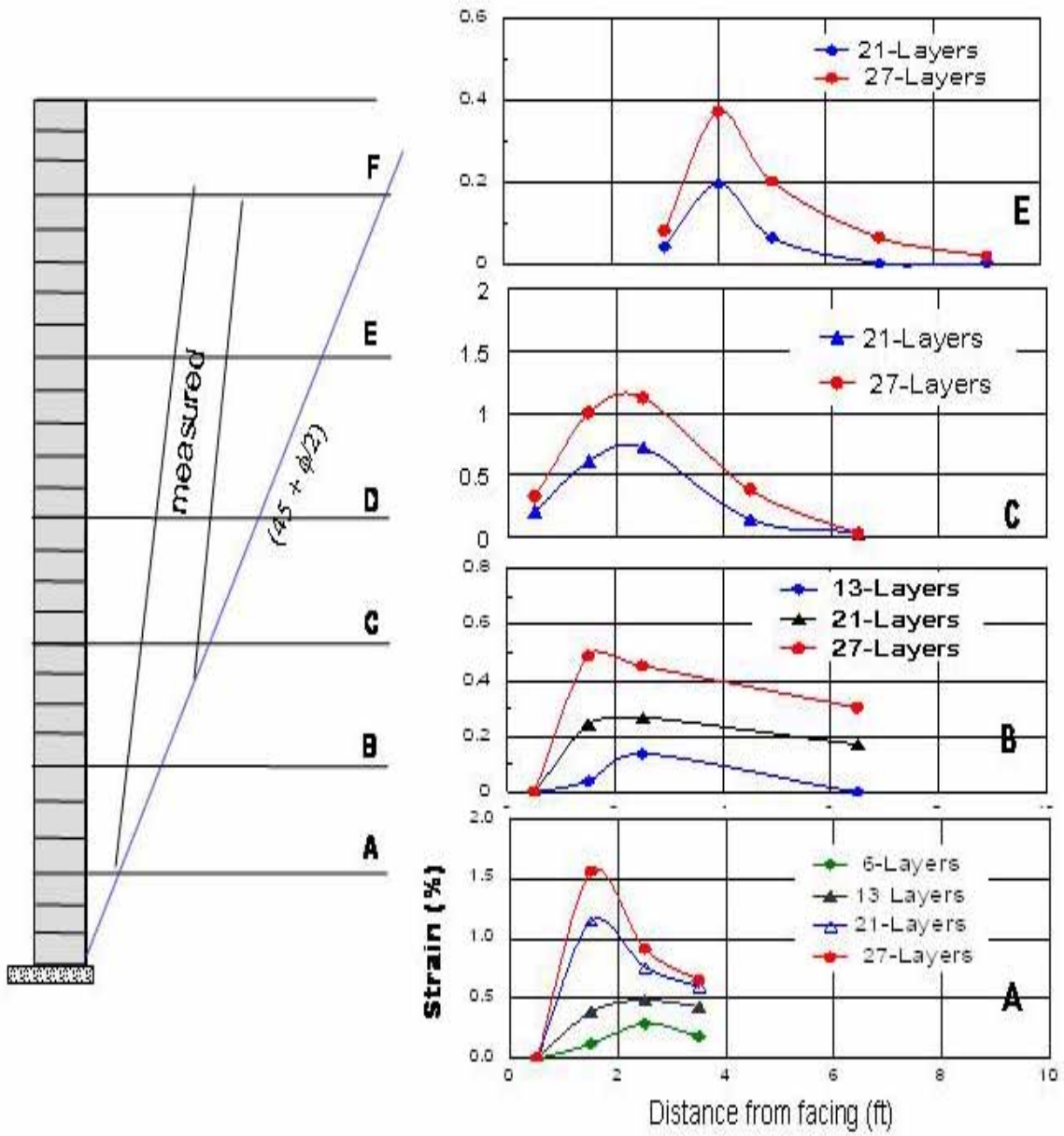


Figure 11 – Strain measurements and locations of maximum strains in test section 3

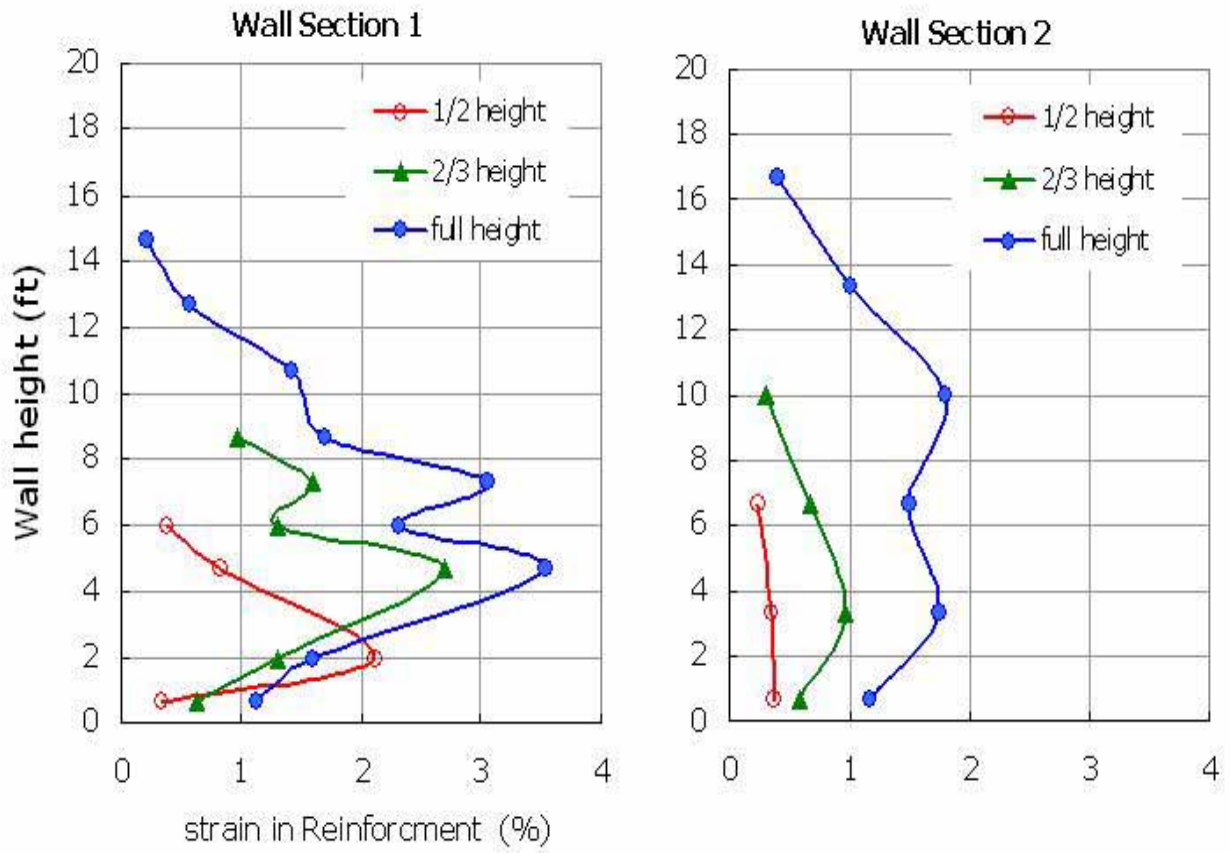


Figure 12 – Magnitudes of maximum strains at various stages of construction

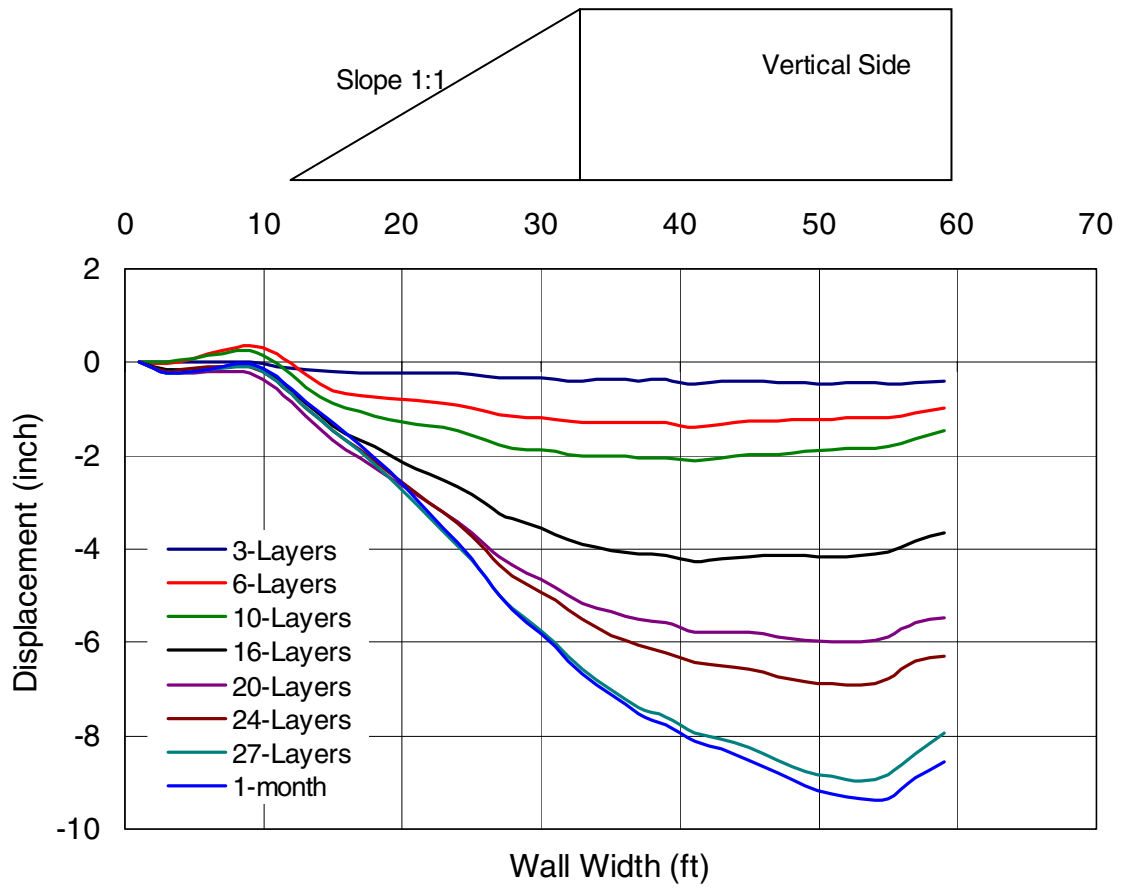


Figure 13 – Settlement profile of the wall from horizontal inclinometer

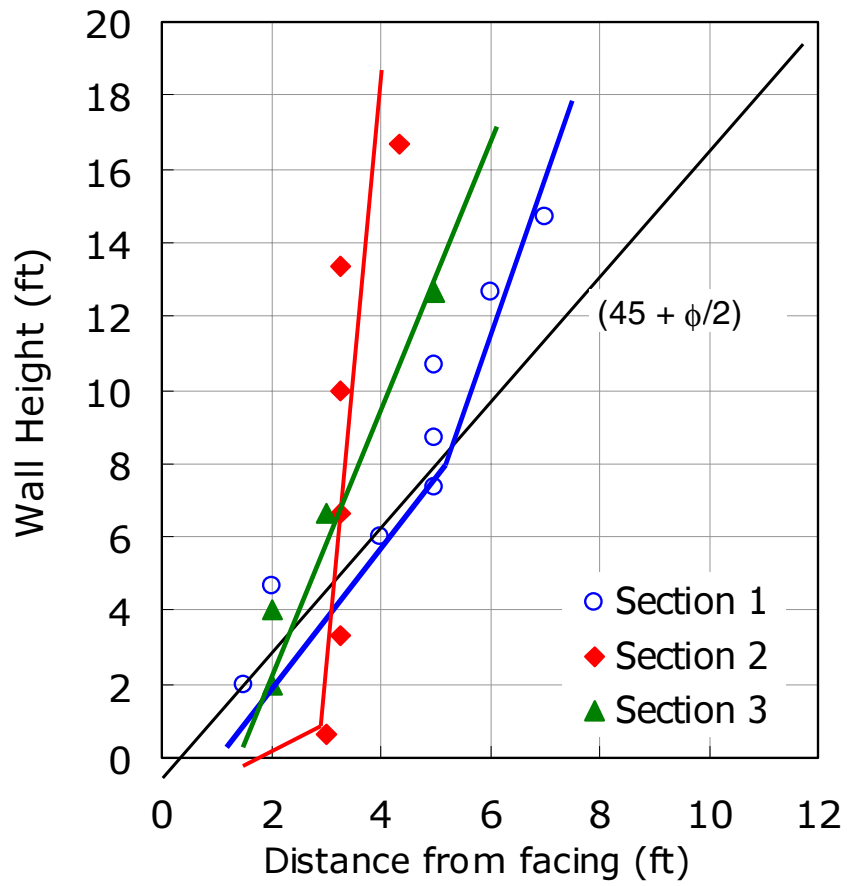


Figure 14- Locations of maximum strains in the test sections

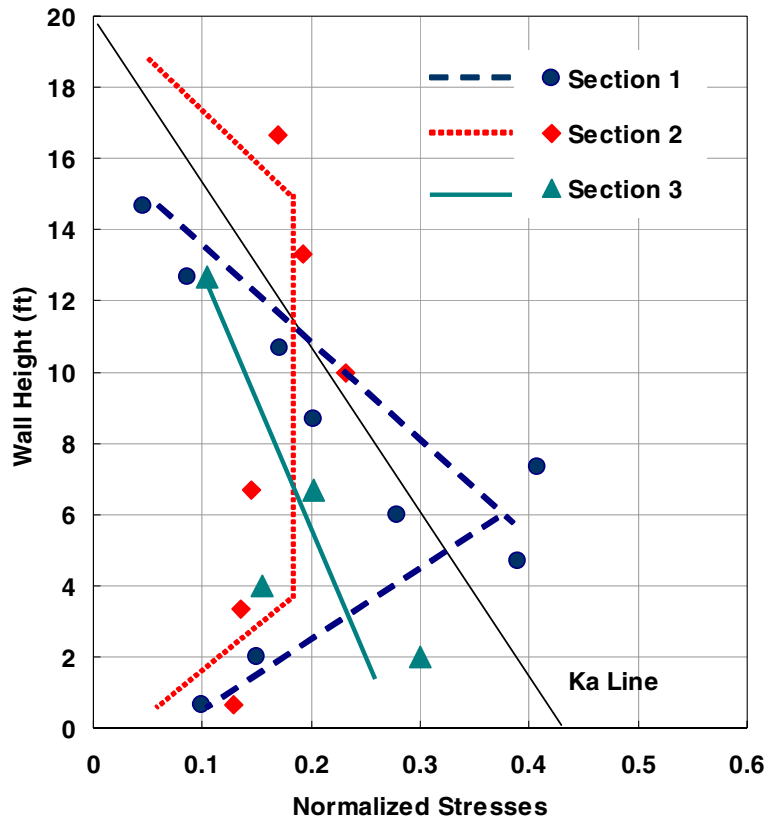


Figure 15 - Locus of maximum stresses in the test sections

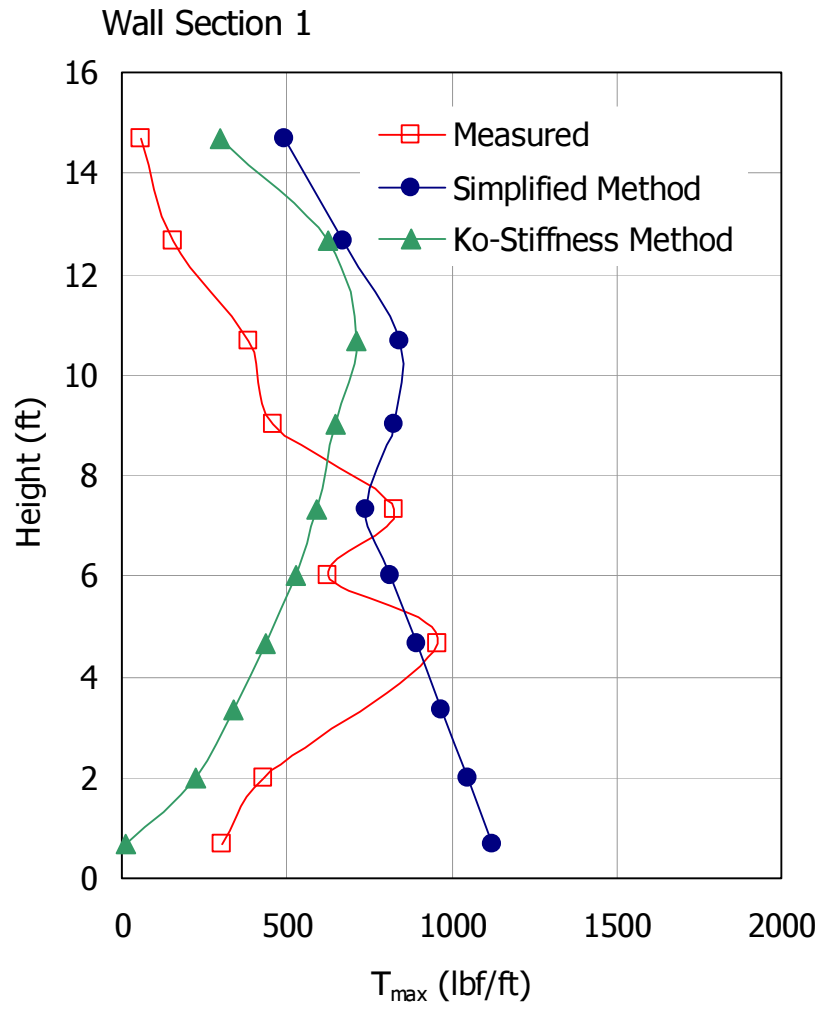


Figure 16 – Measured and theoretical values of T_{max} in wall section 1

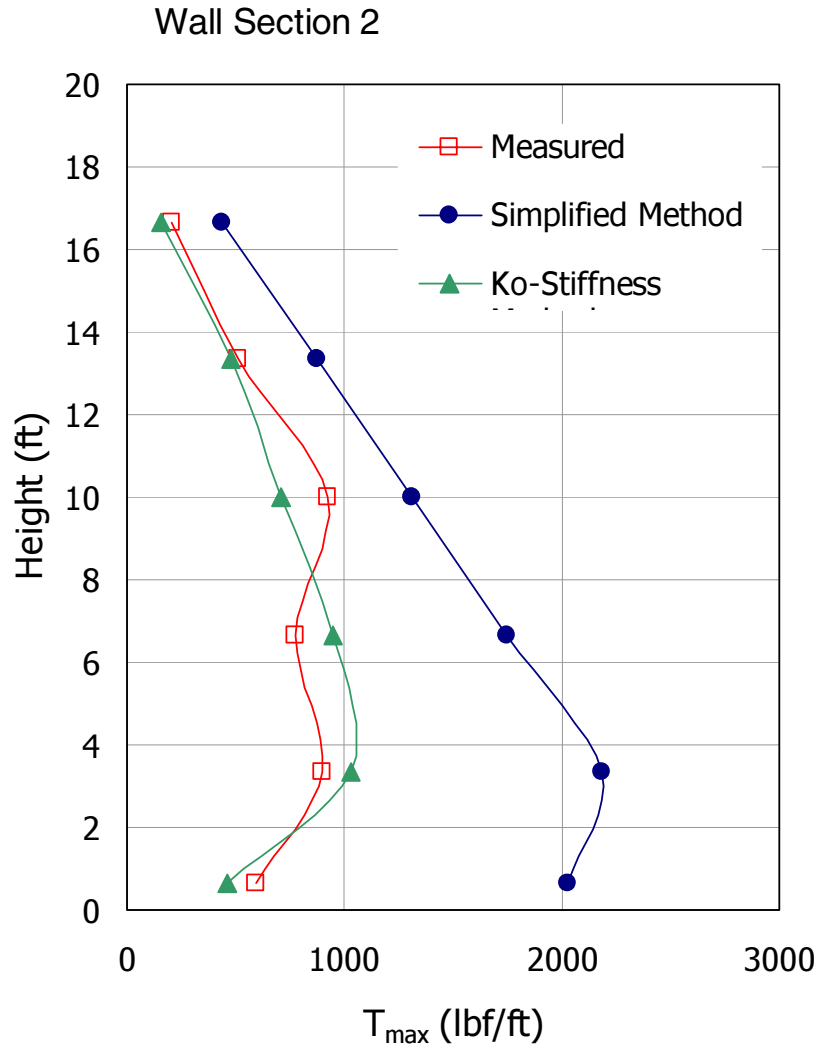


Figure 17 – Measured and theoretical values of T_{max} in wall section 2

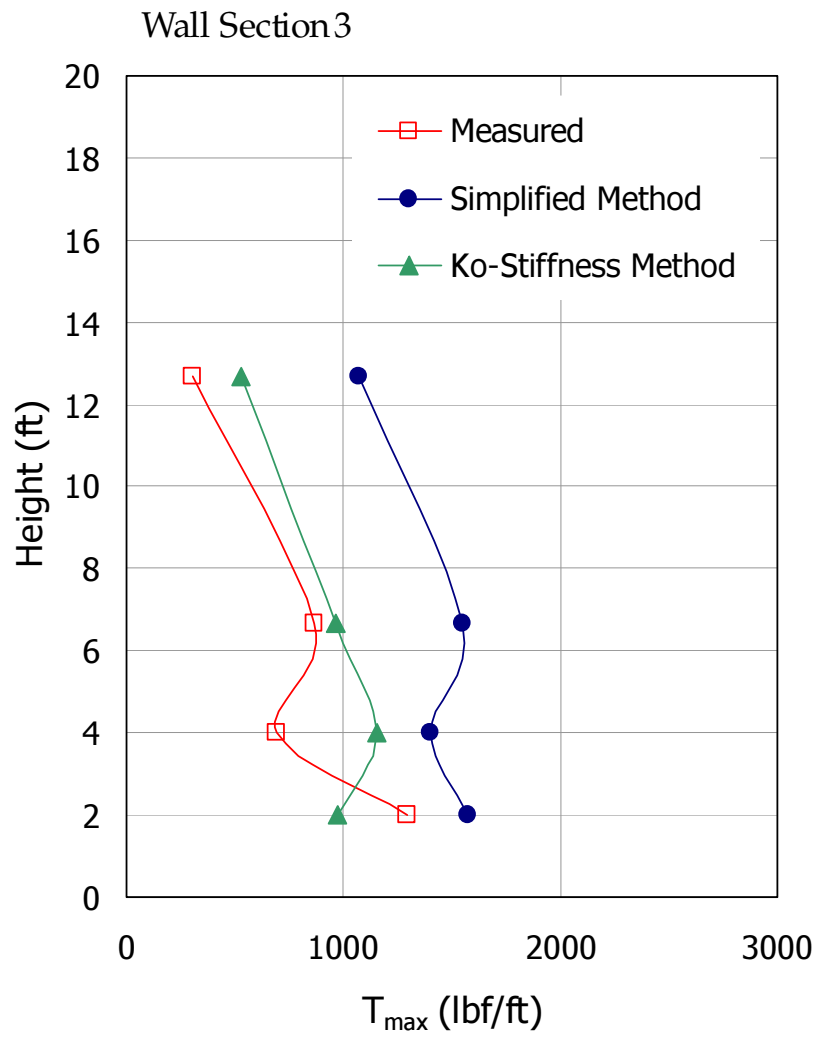


Figure 18 – Measured and theoretical values of T_{max} in wall section 3